

LETTER TO THE EDITOR

Probing the mass and structure of the Ring Nebula in Lyra with SOFIA/GREAT observations of the [CII] 158 micron line

R. Sahai¹, M. R. Morris², M. W. Werner¹, R. Güsten³, H. Wiesemeyer³, and G. Sandell⁴

¹ Jet Propulsion Laboratory, 4800 Oak Grove Drive, Pasadena, CA 91109-8001, USA
e-mail: raghvendra.sahai@jpl.nasa.gov

² Department of Physics and Astrophysics, University of California, Los Angeles, CA 90095-1547, USA

³ Max-Planck-Institut für Radioastronomie, Auf dem Hügel 69, 53121 Bonn, Germany

⁴ SOFIA-USRA, NASA Ames Research Center, MS 232-12, Building N232/Rm. 146, Moffett Field, CA 94035-0001, USA

Received 10 February 2012 / Accepted 26 March 2012

ABSTRACT

We have obtained new velocity-resolved spectra of the [CII] 158 μm line towards the Ring Nebula in Lyra (NGC 6720), one of the best-studied planetary nebulae, in order to probe its controversial 3-dimensional structure and to estimate the mass of circumstellar material in this object. We used the terahertz receiver GREAT aboard the SOFIA airborne telescope to obtain the [CII] spectra at eight locations within and outside the bright optical ring of NGC 6720. Emission was detected at all positions except for the most distant position along the nebula's minor axis, and generally covers a broad velocity range, $\Delta V \sim 50 \text{ km s}^{-1}$ (FWZI), except at a position along the major axis located just outside the optical ring, where it is significantly narrower ($\Delta V \sim 25 \text{ km s}^{-1}$). The one narrow spectrum appears to be probing circumstellar material lying outside the main nebular shell that has not been accelerated by past fast wind episodes from the central star, and therefore most likely comes from equatorial and/or low-latitude regions of this multipolar nebula. Along lines-of-sight passing within about $10''$ of the nebular center, the CII column density is a factor 46 higher than the CO column density. The total mass of gas associated with the [CII] emission inside a circular region of diameter $87''.5$ is at least $0.11 M_{\odot}$. A significant amount of [CII] flux arises from a photodissociation region immediately outside the bright optical ring, where we find a CII to CO ratio of >6.5 , lower than that seen towards the central region. Comparing our data with lower-quality CI spectra, which indicate similarly large CI/CO ratios in NGC 6720, we conclude that the bulk of elemental carbon in NGC 6720 is divided roughly equally between CII and CI, and that the emissions from these species are far more robust tracers of circumstellar material than CO in this object and other evolved planetary nebulae.

Key words. planetary nebulae: individual: NGC 6720 – stars: winds, outflows – photon-dominated region (PDR) – circumstellar matter – planetary nebulae: general

1. Introduction

Planetary nebulae (PNe) result when “ordinary” stars, with main-sequence masses $1\text{--}8 M_{\odot}$, die extraordinary deaths. During their post-main-sequence evolutionary phase (i.e., as AGB stars), these stars eject half or more of their total mass in the form of nucleosynthetically-enriched material into the interstellar medium (ISM) – a process which dramatically alters the course of stellar evolution, and plays a key role in the chemical evolution of the Galaxy. PNe are formed when most of the stellar envelope has been ejected and the hot central star's radiation field ionizes the ejecta.

PNe are almost a unique astrophysical class in terms of being bright at all wavelength bands from X-ray to radio, and are ideal laboratories for investigating important astrophysical phenomena such as nucleosynthesis, (magneto)hydrodynamics of colliding winds, astrochemistry, photodissociation, and the evolution of dust grains (via UV and shock-processing) because their geometries and kinematics are generally believed to be well understood (e.g., Gurzadyan 1997). The history of the mass-loss processes which result in a PN, beginning from its life as an AGB star, is written in the spatio-kinematic structure of the circumstellar ejecta surrounding the central star. Different geometries can require radically different formation models – for example,

in the binary-driven model for aspherical PNe, ellipsoidal shapes result from sub-stellar mass companions, whereas bipolar shapes require interaction with a stellar-mass companion (Soker 1996).

However, inferring the 3D physical structure of a PN from its observed 2D projection on the sky can be a difficult task. This is because PNe appear in a dazzling variety of complex morphologies, with collimated, bipolar and multipolar shapes being dominant, and round ones being rather rare, as clearly seen in imaging surveys with HST (e.g., Sahai & Trauger 1998; Sahai et al. 2011). Furthermore, although PNe shapes have traditionally been defined by optical imaging, the latter typically do not show where the bulk of the mass in these objects lies: in a photodissociation region (PDR) surrounding the bright optical nebula, of up to $\sim 1 M_{\odot}$, compared to $\sim 0.1 M_{\odot}$ in ionized gas (cf., Hollenbach & Tielens 1999). This PDR may represent most of the mass ejected during the AGB phase; some fraction of it is sculpted and compressed by fast post-AGB winds from the central star, resulting in the complex shapes of PNe seen in optical imagery. The bulk of the PDR material radiates most of its energy via thermal emission in the far-infrared.

At a distance of 0.7 kpc, NGC 6720 (M 57), the Ring Nebula in Lyra, is among the brightest and most extensively studied PNe (e.g., O'Dell et al. 2007; ODell07, and references therein, van Hoof et al. 2010). NGC 6720 has an elliptical ring shape

(size $\sim 90'' \times 60''$) in optical emission lines. This bright ring lies at the center of a large “double” halo structure: a brighter inner one (size $\sim 160'' \times 146''$) consisting of a system of limb-brightened loops, and an outer faint one which is irregular, knotty and round ($\sim 230''$ diameter: Balick et al. 1992). Although it is considered a “classical” nebula because of the bright ring’s simple 2D shape, its detailed 3D structure remains controversial, in spite of many studies undertaken to elucidate it (see, e.g., ODell07).

We report here the results of a small program conducted as part of Basic Science observations on the Stratospheric Observatory For Infrared Astronomy (SOFIA), to use velocity-resolved observations of [CII] $158\mu\text{m}$ line emission for probing the mass and 3D structure of NGC 6720. The use of the [CII] $158\mu\text{m}$ line as a probe stemmed from our expectation that, because [CII] is present both in the ionized and atomic components of the circumstellar environment, and because this line has a low critical density ($\lesssim \text{few } 10^3 \text{ cm}^{-3}$), it should be readily observable both within and outside the optically-bright PN ring.

2. Observations

The observations were performed with the (dual-channel) German REceiver for Astronomy at Terahertz frequencies (GREAT¹, Heyminck et al. 2012) onboard SOFIA during three flights with durations of 70, 85 and 60 min on 2011 July 12, July 17, and Sept. 28, at altitudes of 43 000, 43 000 and 41 000 ft, respectively. We used the Fast Fourier Transform spectrometer with 1.5 GHz instantaneous bandwidth (236.6 km s^{-1} at the [CII] line frequency of 1900.5369 GHz). The symmetric beam-switching mode was employed with a throw of $6'$ along the Dec axis. Pointing was accurate to better than $5''$, and the system temperature was $\sim 3950\text{--}4530 \text{ K}$. Spectra of the [CII] line were obtained at eight locations inside and outside NGC 6720’s bright ring along its major and minor axes (Fig. 1), with an angular resolution of $\sim 15''/6$. The data were processed with the latest version of the GREAT calibration pipeline. We reduced the spectra further by boxcar smoothing these to a resolution of 2.888 km s^{-1} and removal of linear baselines. The typical integration time (1σ noise) per position (i.e., excluding the time spent on the “off” positions) ranged between 5–8 min ($0.06\text{--}0.1 \text{ K}$), except for #4, where it was 3.5 min (0.14 K). Using the beam efficiencies $\eta_c = 0.51$ for [CII] and the forward efficiency $\eta_f = 0.95$ (Heyminck et al. 2012), all data were converted to a main-beam brightness temperature scale $T_{\text{mb}} = \eta_f T_{\text{A}}^* / \eta_c$ for computing the total [CII] flux. The temperature scale is uncertain by 20%.

3. Results

We detected emission at all positions except #9, where the rms noise is 0.09 K (Table 1). The emission generally covers a broad velocity range, $\Delta V \sim 50 \text{ km s}^{-1}$ (full-width at zero intensity: FWZI), except at position #4, where it is significantly narrower ($\Delta V \sim 25\text{--}30 \text{ km s}^{-1}$) (Fig. 2). An average spectrum from the central (#1) and four symmetric locations on the major and minor axes (#3, #5, #8, #8a) shows a symmetric profile with a central double-peaked core of width $\Delta V \sim 48 \text{ km s}^{-1}$, centered at $V_{\text{lsr}} = -2.6 \text{ km s}^{-1}$, and a weaker high-velocity pedestal with a total width of about 100 km s^{-1} at its base. The observed width of the high-velocity component is limited by the signal-to-noise,

Table 1. GREAT observations of [CII] in NGC 6720.

Position label	Offset $\Delta\alpha''$, $\Delta\delta''$	$F([\text{CII}])$ K km s^{-1}	$N([\text{CII}])$ 10^{17} cm^{-2}
1	(0, 0) ^a	27.9	1.24
2	(−14.7, −9.5)	15.0	0.67
3	(−29.3, −19.1)	21.8	0.97
5	(+29.3, +19.1)	29.2	1.29
8	(−19.1, +29.3)	22.2	0.98
8a	(+19.1, −29.3)	41.2	1.82
4	(−44.0, −28.6)	12.5	0.55
9	(−28.6, +44.0)	<4.5	0.20

Notes. ^(a) Coordinates are J2000 RA = 18:53:35.08, Dec = 33:01:45.0.

and is likely larger than 100 km s^{-1} (e.g., by folding and averaging this profile around its center velocity, we reduce the noise and find clear evidence for emission extending over 120 km s^{-1}). The line profile towards position #1, although noisy, clearly does not show even a hint of a minimum around the systemic velocity. Since an expanding hollow shell would produce a strong minimum, we conclude that C^+ is not absent from the region interior to the bright ring.

We compute the [CII] column density at different locations in the nebula from the observed [CII] intensity, $I([\text{CII}])$ ($\text{erg s}^{-1} \text{ cm}^{-2} \text{ sr}^{-1}$), using Eq. (A.5) of Schneider et al. (2003), $N([\text{CII}]) = 6.3 \times 10^{20} I([\text{CII}]) \text{ cm}^{-2}$ (Table 1). We have reasonably assumed that the density and temperature are high enough for thermalized emission – the upper level of the [CII] line is 91 K above ground, and the critical densities for collisional excitation by electrons (at $T_e = 8000 \text{ K}$), H, and H_2 are $46, 3 \times 10^3$ and $5 \times 10^3 \text{ cm}^{-3}$, respectively (Stacey et al. 2010; Schneider et al. 2003), to be compared with the electron density in the ionized nebula ($500\text{--}700 \text{ cm}^{-3}$, ODell07), and the density (10^5 cm^{-3}) and temperature (300 K) in the PDR of NGC 6720 (Liu et al. 2001). Hence, with $I([\text{CII}]) = 2 \times 10^{-4} \text{ erg s}^{-1} \text{ cm}^{-2} \text{ sr}^{-1}$ towards the nebular center, we find $N([\text{CII}]) = 1.2 \times 10^{17} \text{ cm}^{-2}$.

Since we have sampled the nebula sparsely with beams separated by $17''.5$, we estimate the total [CII] flux by approximating the [CII] emitting region as a central, circular region of $17''.5$ diameter, surrounded by two concentric annuli. The mean radius of annulus 1 (2) is equal to the offsets of position #2 (#3; same for #'s 5, 8 & 8a) from the center, and each has a width of $17''.5$. We derive the average intensity in each region from the average of the spectra sampling it, and multiply it by the region’s area to derive the flux. We thus find that the total [CII] flux, $F([\text{CII}]) = 2.54 \times 10^{-11} \text{ erg s}^{-1} \text{ cm}^{-2}$. Assuming all of the carbon is in C^+ , that the distance is 0.7 kpc , and taking $\text{C}/\text{H} = 7.9 \times 10^{-4}$ for NGC 6720 (Liu et al. 2001, Table 5), we find that the total mass of gas associated with the [CII] emission inside a circular region of diameter $87''.5$ is at least $0.114 M_\odot$. Our mass estimate is a very conservative lower limit because (i) we have not taken into account the emission from locations beyond the main ring, such as position #4, and (ii) a comparable fraction of carbon is likely to be neutral (see below). We note that Liu et al. (2001) estimated a mass of $0.03 M_\odot$ from their [CII] $158\mu\text{m}$ line flux of $6.8 \times 10^{-12} \text{ erg s}^{-1} \text{ cm}^{-2}$ for NGC 6720, measured using the ISO Long Wavelength Spectrometer (LWS) with a single $\sim 70''$ aperture covering the main optical nebula. Clearly, a significant amount of [CII] flux lies outside the $70''$ ISO/LWS aperture, i.e., in the PDR beyond the main optical nebula.

We compare our [CII] results with those from studies of CO and CI emission in NGC 6720. For CO, Bachiller et al. (1989: BBMG89) have obtained complete maps in the $J = 1\text{--}0$ and $2\text{--}1$ lines, whereas for CI, Bachiller et al. (1994: BHCF94) detect emission in the $609\mu\text{m}$ line with low S/N at

¹ GREAT is a development by the MPI für Radioastronomie and the Universität zu Köln, in cooperation with the MPI für Sonnensystemforschung and the DLR Institut für Planetenforschung.

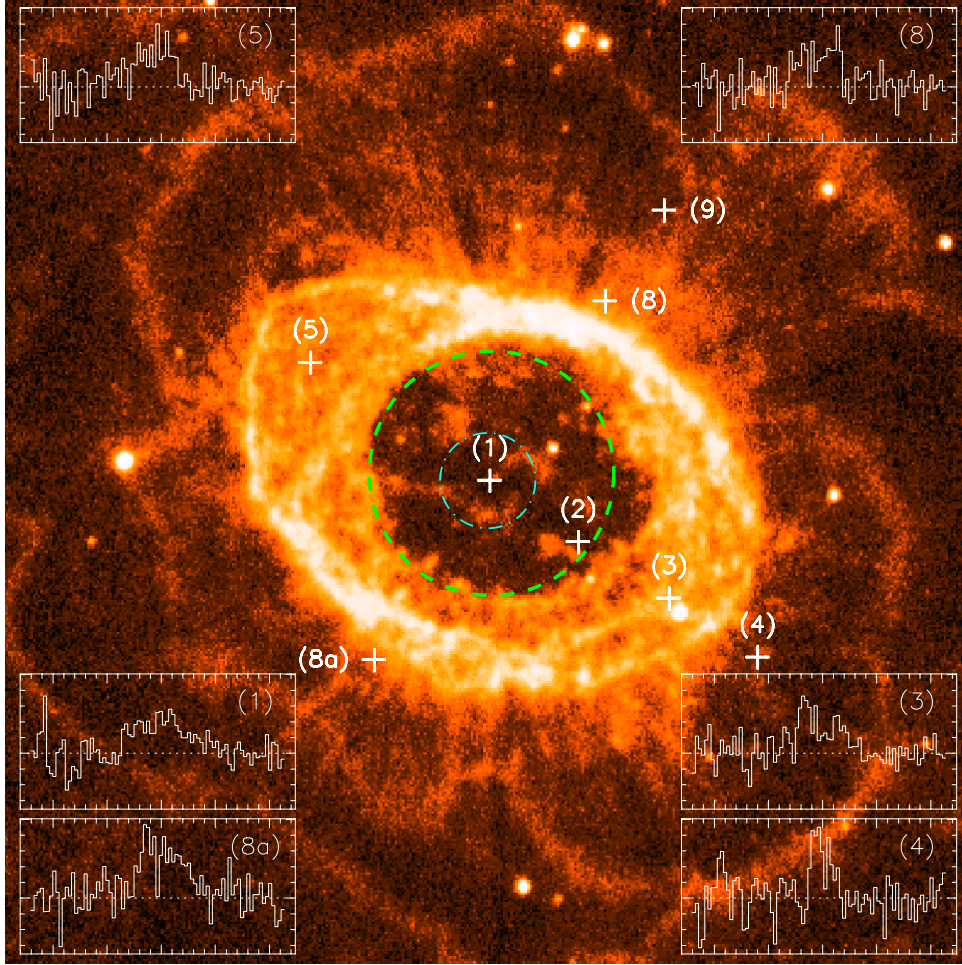


Fig. 1. Spectra of the [CII]158 μ m emission observed with GREAT towards NGC 6720 obtained at different offsets from the center (see Table 1), overlaid on a 157'9 \times 157'9 H₂ 2.1 μ m image (taken by David Thompson). The positions of the 15'6 GREAT beam, shown in cyan at the center (J2000 RA = 18:53:35.08, Dec = 33:01:45.0) are marked by crosses. The small tick marks are separated by 10 km s⁻¹ on the velocity axis (V_{lsr}), and by 0.1 K on the intensity axis (T_A^*). The spectrum at position #4 has been scaled by a factor 0.75. The equator of the multipolar model we propose for NGC 6720 is shown by the green dashed circle with diameter 40'.

a few (3 of 5) positions along the minor axis. The CO and CI column densities towards the nebular center are $N(\text{CO}) = 2.6 \times 10^{15} \text{ cm}^{-2}$ (BBMG89) and $N(\text{CI}) \sim 10^{17} \text{ cm}^{-2}$ (BHCF94). Hence, both the CII/CO and the CI/CO abundance ratios are about 50 towards the nebular center, i.e., almost all of the nebular carbon is distributed roughly equally between C⁺ and C. Towards positions offset from the nebular center, the CII/CO abundance ratio, while still large, is not as extreme. We find (i) $N(\text{CII}) = 5.5 \times 10^{16} \text{ cm}^{-2}$ towards position #4, and (ii) $N(\text{CO}) = 8.4 \times 10^{15} \text{ cm}^{-2}$ near position #4 from BBMG89's CO $J = 2-1$ map, using their spectrum at offset position ($\Delta\alpha, \Delta\delta = -40'', -20''$). Since this spectrum (obtained with a 13'' beam) samples the strongest emission peak in the CO map, whereas our #4 spectrum (15'6 beam), is offset by 9'5 from that peak, our derived C⁺ to CO ratio here is at least 6.5. Our CII study strongly supports the hypothesis that the CO emission region in NGC 6720 is really a PDR (BHCF94). We note that the CO $J = 2-1$ emission shows significant clumpy structure, and given the strong [CII] emission seen at position #4 where the CO emission is also strong, and the lack of [CII] emission at #9 (3σ upper limit of $N(\text{CII}) < 2 \times 10^{16} \text{ cm}^{-2}$ assuming same velocity width as at position #4), where the CO emission is very weak, it is likely that the [CII] is similarly clumpy.

Noting that the CII column densities at all positions we have sampled in NGC 6720 (Table 1) exceed the maximum

CO column density in NGC 6720 by large factors, and that the average CI/CO ratio is 10 (BHCF94), we conclude that CII and CI are far more robust tracers of circumstellar mass in this object than CO. If we assume that the abundances of CII and CI are roughly equal, then our circumstellar mass estimate from [CII] data increases to $>0.23 M_{\odot}$. Hence, given estimates of the current central star mass of 0.61–0.62 M_{\odot} (Odell07), and that the mass of the outer halo has not been accounted for, it is likely that the mass of NGC 6720's progenitor star exceeded 1 M_{\odot} .

3.1. Structure

Models for the 3D structure of NGC 6720 can be divided into two broad classes. The first (model 1) is a (roughly) prolate ellipsoid, having open ends along the long axis: thus a barrel shape, with an equatorial density enhancement and the axis of symmetry inclined at 30° to the line of sight (Masson 1990; Guerrero et al. 1997; GMC97). This model has been refined by Hiriart (2004) and Odell07 (using mapping of the 2.1 μ m H₂ line, and multislit optical spectra, respectively) to one in which the barrel cross-section is elliptical and it is seen nearly pole-on. In the second class of models (model 2), NGC 6720 is seen as a nearly pole-on bipolar nebula based on multislit spectra along the major axis (Bryce et al. 1994). Kwok et al. (2008) compare deep emission-line images of NGC 6720 with another well-studied PN, NGC 6853, and suggest that both have the same

biconical 3D structure, except that NGC 6853 is oriented edge-on, whereas NGC 6720 is nearly pole-on. In the Kwok et al. (2008) model, the inner and outer halo together represent the projections of three pairs of bi-conical outflows with similar opening angles, viewed along their common symmetry axes. From their CO $J = 2-1$ study, BBMG89 infer a structure which has elements of both class 1 and class 2: a hollow cylindrical shape with its axis inclined to the line-of-sight.

We propose that NGC 6720 is a PN with a barrel-shaped central region viewed (nearly) along its axis, which can reconcile the above model classes. Barrel-shaped central regions have recently been recognized as an important feature of many PNe in a comprehensive new morphological classification system based on HST images of 119 young PNe by Sahai et al. (2011). NGC 6720 is also multipolar, with the “flower-petal” structures in the H_2 and [NII] images seen in the “inner halo” of NGC 6720 being the limb-brightened peripheries of these lobes. The presence of such lobes is also indicated by the appearance of multiple, faint, red- and blue-shifted velocity components within the overall position-velocity ellipse seen in optical long-slit spectra reported by GMC97 and interpreted as resulting from “bubbles of material (that) protrude from the main nebula”. The NGC 6720 ring shows several extended filamentary structures which suggests that a significant fraction of the ring’s optical line emission comes from the bright basal regions of multiple lobes emanating from the central region; the continuation of these regions to slightly higher latitudes is seen in the fainter, more diffuse, emission in the H_2 image immediately outside the bright ring (Fig. 1). This suggestion finds support in GMC97’s finding that “the velocity structure of the edge of the nebula shows a complex behaviour”, “reflecting the projected velocity of these clumps and bubbles”. Optical spectra of the flower-petal region (Fig. 8 of GMC97) show distinct narrow components separated by $\sim 25-30 \text{ km s}^{-1}$. In our model, these result from the inclined walls of lobes on the near- and far-side of the equatorial plane. These spectra also show the presence of point-symmetric pairs of knotty structures which are consistent with an origin in oppositely-directed multiple outflows, rather than bubbles created by a fast wind flowing through a fragmented shell as GMC97 propose, because it is very unlikely that a stochastic process (fragmentation) can create point-symmetrically located holes in a shell. The multipolar PN He 2-47 (Sahai 2000) provides us a rough idea of what NGC 6720’s lobes might look like if the symmetry axis of its central barrel was in (or nearly in) the sky-plane.

Although a detailed interpretation of all the published data on NGC 6720 with our proposed model is outside the scope of this paper, our [CII] data appear consistent with this model, provided the lobes are expanding at similar velocities. In this model, the [CII] emission at positions 3, 5, 8, and 8A, which likely includes emission from both the barrel-shaped central region and low-latitude regions of multipolar lobes, is expected to be roughly similar, as observed. The spectrum at position #4 provides insight into the circumstellar material that lies outside the main nebular ring and whose physical properties are not well known – the narrow profile ($\Delta V \sim 25 \text{ km s}^{-1}$) suggests that the [CII] emission is probing material that has not been accelerated by past fast wind episodes from the central star, and therefore most likely comes from equatorial and low-latitude regions of the slowly-expanding progenitor AGB wind. In contrast, the emission from positions #8 and #8a which, like that from #4, also samples material largely just outside the shell’s periphery but along the minor axis, is broad ($\Delta V \sim 40-45 \text{ kms}$) and may

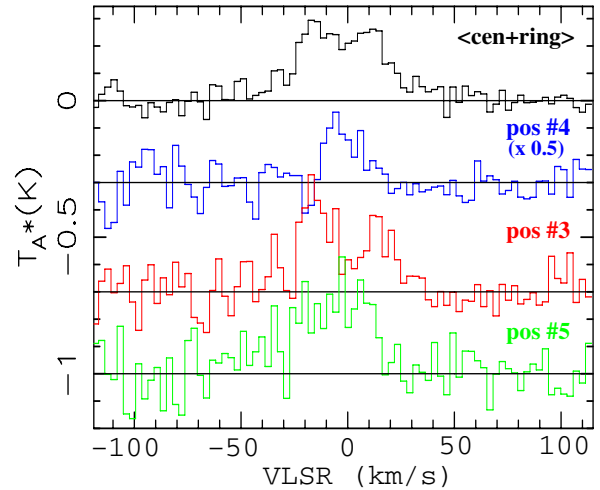


Fig. 2. [CII] spectra obtained at specific locations in NGC 6720 with GREAT. The #4 (rescaled by 0.5), #3, and #5 spectra have been shifted vertically by -0.3 , -0.7 , and -1.0 K for clarity. The “cen+ring” spectrum is an average of broad spectra found at the central (position #1) and four symmetric locations on the major and minor axis (positions #3,#5,#8,#8a).

be associated with the multipolar lobes whose peripheries show up in projection as the “flower-petals” in the H_2 image (Fig. 1).

In summary, our results show that for NGC 6720 (and by inference other evolved PNe), C^+ is a much more robust tracer of the circumstellar material than CO because it is far more abundant. We therefore expect future GREAT [CII] observations to play a major role in the study of evolved PNe.

Acknowledgements. This study is based on observations made with the NASA/DLR Stratospheric Observatory for Infrared Astronomy (SOFIA). SOFIA Science Mission Operations is operated by the Universities Space Research Association, Inc., under NASA contract NAS2-97001, and the Deutsches SOFIA Institut under DLR contract 50 OK 0901. R.S.’s contribution to the research described here was carried out at the Jet Propulsion Laboratory, California Institute of Technology, under a contract with NASA. Financial support was provided by NASA through a Long Term Space Astrophysics award to R.S. and M.M., and a SOFIA award to R.S.

References

- Bachiller, R., Bujarrabal, V., Martin-Pintado, J., & Gomez-Gonzalez, J. 1989, A&A, 218, 252 (BBMG89)
- Bachiller, R., Huggins, P. J., Cox, P., & Forveille, T. 1994, A&A, 281, L93 (BHCF94)
- Balick, B., Gonzalez, G., Frank, A., & Jacoby, G. 1992, ApJ, 392, 582
- Bryce, M., Balick, B., & Meaburn, J. 1994, MNRAS, 266, 721
- Guerrero, M. A., Manchado, A., & Chu, Y.-H. 1997, ApJ, 487, 328 (GMC97)
- Gurzadyan, G. A. 1997, The Physics and Dynamics of Planetary Nebulae, XVI (Springer-Verlag)
- Heyminck, S., Graf, U., Güsten, R., et al. 2012, A&A, 542, L1
- Hiriart, D. 2004, PASP, 116, 1135
- Hollenbach, D. J., & Tielens, A. G. G. M. 1999, Rev. Mod. Phys., 71, 173
- Kwok, S., Chong, S.-N., Koning, N., Hua, T., & Yan, C.-H. 2008, ApJ, 689, 219
- Liu, X.-W., Barlow, M. J., Cohen, M., et al. 2001, MNRAS, 323, 343
- Masson, C. R. 1990, ApJ, 348, 580
- O’Dell, C. R., Sabbadin, F., & Henney, W. J. 2007, AJ, 134, 1679 (ODell07)
- Sahai, R. 2000, ApJ, 537, L43
- Sahai, R., & Trauger, J. T. 1998, AJ, 116, 1357
- Sahai, R., Morris, M. R., & Villar, G. G. 2011, AJ, 141, 134
- Schneider, N., Simon, R., Kramer, C., et al. 2003, A&A, 406, 915
- Soker, N. 1996, ApJ, 460, L53
- Stacey, G. J., Hailey-Dunsheath, S., Ferkinhoff, C., et al. 2010, ApJ, 724, 957
- van Hoof, P. A. M., van de Steene, G. C., Barlow, M. J., et al. 2010, A&A, 518, L137